LINE PHOTOGRAMMETRY WITH MULTIPLE IMAGES

Author: Dipl. Ing. Holger Zielinski
Institution: Dept. for Photogrammetry
Address: The Royal Institute of Technology
S-100 44 Stockholm
Country: Sweden
Commission Number: III

ABSTRACT

A method for the calculation of 3D point coordinates from the combination of 3D straight lines, called line photogrammetry, will be presented. It is partly based on already existing theory. The 3D straight lines are directly calculated from non homologous points identified in multiple images by manual registration. Four parameters are used to define a 3D straight line. Space lines do not in general intersect due to errors in orientation and measurements. The solution used here is to include an intersection constraint into the least squares adjustment or to find a point with a shortest distance to the lines. For the tests, two buildings are measured in aerial photographs by using both stereo and line photogrammetry, and geodetically as reference. The evaluation of the results showed that line photogrammetry has the same or higher precision compared with stereo photogrammetry. More extensive tests need to be done, before this statement can be generalized.

Key words: precision, 3-D, features, multi-image

1. INTRODUCTION

In digital photogrammetry, it is already possible to do the whole image orientation fully automatic. Even the generation of digital elevation models has reached a high degree of automation. The majority of methods for automation are point oriented.

For map production the automatic reconstruction of the shape of man-made objects and their precise localisation is of importance. The corner points of a building can be used to describe its shape. In a production process these points are manually measured by an operator. Automating this process means, that those image points have to be selected automatically which represent the same corner point in object space. Here the well known point correspondence problem have to be solved.

Instead of describing an object by corner points, it can also be described using lines, i.e. the line between a roof and a wall of a building. Such object lines can be described with the help of linear features. The parameters of such 3D linear features can be calculated using an arbitrary number of measured image points describing the feature.

Line photogrammetry is the formulation of a direct mathematical relation between measured image points and the parameters of a 3D linear feature. The advantage of using line photogrammetry instead of point oriented photogrammetry is, that no stereo point to point relation is necessary. The parameters of a feature can be calculated using measured image points form different parts of the projected 3D feature. The only constraint which have to be fullfilled is, that the measured images points belong to the same 3D linear feature.

A few published works exist which combine photogrammetry and linear features. Masry [2] described a method for absolute camera orientation and Lugnani [1] for camera orientation by spatial resection, using linear features.

Persson [4] developed these ideas further, so that it was possible to calculate the parameters of a 3D straight line in object space directly from monoscopically measured image points.

Mulawa and Mikhail [3] expanded the method in such a way that more general objects like circles, ellipses or splines could be used as linear features. They made the point that this method can be used as a tool for the development of automatic measurement procedures. The parameters of the linear features were geometrically understandable, but dependent of each other.

Sayed and Mikhail [5] tested methods for automatic orientation of stereo images and localisation of circular and straight linear features in 3D object space. One of the interesting subject mentioned was to use independent instead of dependent parameters to describe linear features.

The overall purpose of this work is to test, if the use of line photogrammetry will lead to a real improvement for large scale map updating. In this investigation a set of four parameters defining a 3D straight linear feature are introduced. The reason to use four instead of six dependent parameters is to avoid problems concerning real or numerical singularities and the advantage that no additional geometric constraints have to be introducted explicitly to get a solution. Another intention in the theoretical part of this project is the introduction of geometric constraints for each separate line and between several lines. A theory for 3D straight line linear features, here also called line features or straight lines, is formulated. Furthermore test results are presented, where this method is compared with stereo photogrammetry. The results from a geodetic measuring method are used as references.

2. METHOD

2.1 Basic mathematic relation for a straight line

An arbitrary point on an endless 3D straight line can be expressed by the parametric line equation given in equation (1)

$$P = S + t * d \qquad (1)$$

P is an arbitrary point and S is a fixed point on the line, d is the direction vector of the 3D line and t is a scalar factor. The endless 3D line is totally described with the six dependent parameters, X_S, Y_S, Z_S and X_d, Y_d, Z_d. Point S can be arbitrary chosen, the same is possible for the length of the vector d. This means that two additional constraints are necessary to get an unique solution for the endless line. Person [4] and Mulawa [3] chose the constraint $|d| = 1$, which requires that the length of the direction vector d is unique. Secondly the point S is defined in such a way, that the radius vector to point S and direction vector d are perpendicular. This is realised by setting the scalar product $(d \cdot S)$ to zero.

Mulawa [3] introduced a coplanarity condition in object space as link between the inner and outer orientation elements of the image, the image coordinates of an arbitrary line point and the unknown line parameters. This relation is expressed by equation (2) and shown graphically in figure (1).
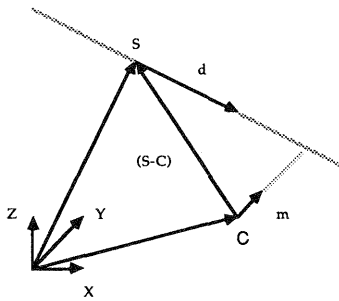
Figure 1: shows the coplanarity constraint which combines the 3D straight line, the image measurements and the orientation parameters of the images.

$$|S\text{-}C, d, m| = 0 \qquad (2a)$$

$$m = R^t \begin{pmatrix} x \\ y \\ -c \end{pmatrix} \qquad (2b)$$

The projection centre of the camera in cartesian ground coordinate system is represented by C and m is a vector including the measured image coordinates of an arbitrary point transformed into a coordinate system parallel to the ground coordinate system. This transformation is done by the rotation matrix R^t.

2.2 Four straight line parameters

The fact that the parameters (X_S, Y_S, Z_S, X_d, Y_d, Z_d) of a straight linear feature are dependent cause some disadvantages. Numerical problems may arise in an overestimated case, where a least square adjustment algorithm is used to calculate the line parameters. There exist two possible reasons. First, the size of the matrices used in the adjustment process get larger and second the a posteriori covariance matrix of the unknown line parameters is singular. On the other hand there are two advantages using the parametric straight line equation and the coplanarity constraint presented in chapter 2.1. They prevent the possibility of a geometric interpretation of the results. Second, the noise

parameters, the scalar factor t and the coordinates of point P are isolated from the process.

Due to the reasons described, an alternative solution will be introduced using four straight line parameters. These parameters still allow the use of the coplanarity formulation as link between image measurements and the 3D line. This means that the parameters S and d have to be expressed as functions of four preliminary parameters A, B, C, D until the final parameters are defined.

$$|S(A, B, C, D)\text{-}C, d(A, B, C, D), m| = 0 \qquad (3)$$

In a cartesian system the point S on the 3D line can be described by the two angles δ, ϕ and the distance r. δ is the angle between the Z-axis and the radius vector to points S. ϕ is the angle between the X-axes and the projection of the radius vector to S onto the X-Y-plane and r is the distance from origo O to point S.

Using δ, ϕ and r the cartesian coordinates of the point S are expressed by

$$X_S = r \sin\delta \cos\phi \qquad (4a)$$

$$Y_S = r \sin\delta \sin\phi \qquad (4b)$$

$$Z_S = r \cos\delta \qquad (4c)$$

To obtain the fourth line parameter, a spherical coordinate system is defined with its origo in point S and the three orthonormal base vectors (e_δ, e_ϕ, e_r).
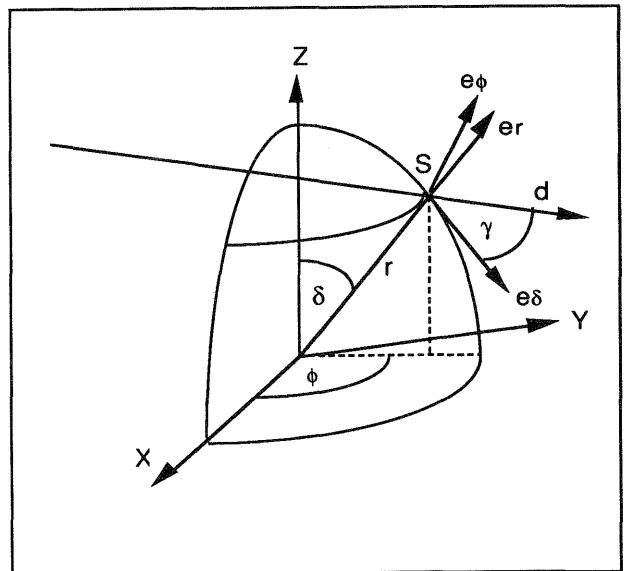
Figure 2 : Point S and vector d expressed by the four parameters δ, ϕ, r, γ.

The vector e_δ is the tangent to the meridian going through S. Vector e_ϕ is the tangent to the parallel circle through point S and vector e_r is the normal vector of the plan (e_δ, e_ϕ) defined by the cross product ($e_\delta \times e_\phi$).

From the definition of e_r follows, that the direction vector d of the straight line will always lie in the (e_δ, e_ϕ)-plane. Angle γ, which is defined as the angle between the e_δ-axes and the direction vector d in the e_δ-e_ϕ-plan is used as the fourth parameter. Figure 2 shows the final geometric relations.

The rotation matrix

$$T_{SC} = \begin{pmatrix} \sin\delta\cos\phi & \cos\delta\cos\phi & -\sin\phi \\ \sin\delta\sin\phi & \cos\delta\sin\phi & \cos\phi \\ \cos\delta & -\sin\delta & 0 \end{pmatrix}, \quad (5)$$

transforms spherical coordinates (S) into cartesian (C) ones. Using the transformation matrix T_{SC}, direction vector d can be express as a function of δ, ϕ, γ,

$$\begin{pmatrix} X_d \\ Y_d \\ Z_d \end{pmatrix} = T_{SC} \begin{pmatrix} 0 \\ l_d * \cos\gamma \\ l_d * \sin\gamma \end{pmatrix} \quad (6)$$

where $l_d = 1$ is the length of d. The point S and the direction vector d are now expressed as functions of the three spherical coordinates δ, ϕ, r and the angle γ.

Now it is possible to exchange the temporary line parameters (A, B, C, D) by (δ, ϕ, r, γ) , i.e. equation (3) is changed to

$$| S(\delta, \phi, r) - C, d(\delta, \phi, \gamma), m | = 0 \quad (7)$$

Describing a straight line with the four parameters δ, ϕ, r, γ results in the explicit analytical equations given in equations (4) and (6).

2.3 Geometric constraints

Man-made objects are often characterized by straight lines. They can be vertical, horizontal, parallel to each other or they can intersect in a point. Therefore the introduction of geometric constraints seems reasonable.
In a first group geometric conditions for one straight linear feature and in the second group constraints concerning two ore more linear features are presented.

First Group of constraints - Independent lines The condition horizontal means, that the direction vector d must be parallel to the X-Y-plan. The e_ϕ-axis is by definition parallel to the X-Y-plan, therefore angle γ must be set to $\gamma = 50$ gon or $\gamma = 150$ gon.
In the vertical case the angle δ have to be set to $\delta = 100$ gon. Therefore the e_δ-axis is parallel to the Z-axes. This leads to the second condition necessary to achieve a vertical line, $\gamma = 0$ gon or $\gamma = 200$ gon.
The last constraint in this group is a chosen angle between the direction vector d_i of the searched line

feature and a known direction d. The chosen angle α between the two direction vectors can be calculated by

$$\cos\alpha = \frac{d_i \bullet d}{|d_i| \, |d|} \quad (8)$$

If direction vector of the searched straight line has index i and the fixed direction d has no index, d_i can be expressed as

$$|d_i| \, |d| \, (\cos\alpha - (a + b + c)) = 0 \quad (9)$$
where
$$a = (\cos\delta_i \cos\phi_i \cos\gamma_i - \sin\phi_i \sin\gamma_i) X_d$$
$$b = (\cos\delta_i \sin\phi_i \cos\gamma_i + \cos\phi_i \sin\gamma_i) Y_d$$
$$c = (-\sin\phi_i \cos\gamma_i) Z_d$$
$$|d_i| = |d| = 1 \text{ length of the two vectors.}$$

The constraints, parallel and perpendicular, are also achieved in this case by setting the angle $\alpha = 0$ gon and $\alpha = 100$ gon respectively.
The condition for the parallel case will look like

$$|d_i| \, |d| \, (1 - (a + b + c)) = 0 \quad (10)$$

and for the perpendicular case

$$|d_i| \, |d| \, (a + b + c) = 0 \quad (11)$$

The help variables (a, b, c) in (10) and (11) are identical with them used in (9).

Second Group of constraints - dependent lines In the first constraint the angle α between two straight line features is chosen. Here two variable 3D straight lines are used. The direction vector of the first line is denoted to d_i, while the second line is denoted to d_{i+1}. New conditions are formulated based on (8). The help variables a,b,c are changed to e,f,g.

$$|d_i| \, |d_{i+1}| \, (\cos\alpha - (e + f + g)) = 0 \quad (12)$$
where
$$e = (\cos\delta_{i+1} \cos\phi_{i+1} \cos\gamma_{i+1} - \sin\phi_{i+1} \sin\gamma_{i+1})$$
$$* (\cos\delta_i \cos\phi_i \cos\gamma_i - \sin\phi_i \sin\gamma_i)$$

$$f = (\cos\delta_{i+1} \sin\phi_{i+1} \cos\gamma_{i+1} + \cos\phi_{i+1} \sin\gamma_{i+1})$$
$$* (\cos\delta_i \sin\phi_i \cos\gamma_i + \cos\phi_i \sin\gamma_i)$$

$$g = (-\sin\phi_i \cos\gamma_i)(-\sin\phi_{i+1} \cos\gamma_{i+1})$$

If the two lines should be parallel then (12) becomes

$$|d_i| \ |d_{i+1}| \ (1-(e+f+g)) \ = \ 0 \qquad (13)$$

and for perpendicular lines we get

$$|d_i| \ |d_{i+1}| \ (e+f+g) \ = \ 0 \qquad (14)$$

Two lines will intersect in a point, if the coplanary constraint

$$|\ (S_2-S_1),d_1,d_2\ | \ = \ 0 \qquad (15)$$

is fullfilled. The last constraint is the intersection of more than two lines in a point. The coplanarity constraint (15) is not sufficient when three or more lines have to intersect in one point. A point P on a line is described by

$$P \ = \ S_i + t_i \ d_i \qquad (16)$$

where $i \ = \ 1,...,n$ and n is the number of lines intersecting in point P. To describe the point P common to all lines, (n-1) conditions are necessary:

$$
\begin{aligned}
S_1 + t_1 \ d_1 &= S_2 + t_2 \ d_2 \\
S_1 + t_1 \ d_1 &= S_3 + t_3 \ d_3 \\
&" \\
&" \\
S_1 + t_1 \ d_1 &= S_i + t_i \ d_i
\end{aligned}
\qquad (17)
$$

The main difference between the conditions in (17) and all others, is the introduction of the new parameters t_i. The scalars t_i locate the intersection point P on each line L_i. Point $S = f(\delta,\phi,r)$ and direction $d = f(\delta,\phi,\gamma)$.

3. ADJUSTMENT PROCESS

For the calculation of the four line parameters a minimal number of four measured image points in at least two images are necessary. Normally much more than these four points will be measured. This leads to an overdetermined problem, which can be solved by a general least square adjustment method. The copla-general least square adjustment method. The coplanarity relationship (7) gives one condition equation for each measured image point. This relationship is non-linear and a function of the measured image coordinates x y of each image line point and the four unknowns δ, ϕ, r, γ :

$$F \ = \ f\ [\ S(\delta,\phi,r)\ ,\ d(\delta,\phi,\gamma)\ ,\ m(x,y)\ ] \qquad (18)$$

Equation (18) is linearised by a Taylor serie using only the linear terms. The linearised coplanarity condition looks

$$F_0 + \left(\frac{\partial F}{\partial x}\right)dx + \left(\frac{\partial F}{\partial y}\right)dy + \left(\frac{\partial F}{\partial \delta}\right)d\delta$$
$$+ \left(\frac{\partial F}{\partial \phi}\right)d\phi + \left(\frac{\partial F}{\partial r}\right)dr + \left(\frac{\partial F}{\partial \gamma}\right)d\gamma = 0 \qquad (19)$$

Expressing the unknown residuals (dx, dy) of the measurements by vector Δl, the parameter corretions ($d\delta$, $d\phi$, dr, $d\gamma$) by vector Δx and using a matrix formulation results in

$$B^t \Delta l \ + \ A_1 \ \Delta x \ + \ w_1 \ = \ 0 \qquad (20)$$

where
$$B^t \ = \ (\ \frac{\partial F}{\partial x}\ ,\ \frac{\partial F}{\partial y}\ )\ ;$$
$$A_1 \ = \ \left(\ \frac{\partial F}{\partial \delta}\ ,\ \frac{\partial F}{\partial \phi}\ ,\ \frac{\partial F}{\partial r}\ ,\ \frac{\partial F}{\partial \gamma}\ \right)\ ;$$
$$w_1 \ = \ B^t \ \overset{o}{l} \ + \ A_1 \ \overset{o}{x}\ ;$$

Vector $\overset{o}{l}$ contains the measured image coordinates and vector $\overset{o}{x}$ the approximated parameters. Assuming that the measurements are normal distributed and not correlated a diagonal weight matrix P is introduced. The introduction of geometric constraints, concerning separate lines investigated in chapter (2.3), leads to an expansion of the least square model (20) with

$$A_2^t \ \Delta x \ + \ w_2 \ = \ 0 \qquad (21)$$

Finally we get

$$B^t \Delta l \ + \ A_1 \ \Delta x \ + \ w_1 \ = \ 0 \qquad (22a)$$

$$A_2^t \ \Delta x \ + \ w_2 \ = \ 0 \qquad (22b)$$

The matrix A_2^t include the derivations of one or several of the equations from chapter 2.3 with respect to $d\delta$, $d\phi$, dr, $d\gamma$. The solution of this adjustment problem is

$$\begin{pmatrix} \Delta x \\ k_2 \end{pmatrix} = \begin{pmatrix} -N & | & A_2 \\ A_2^t & | & 0 \end{pmatrix}^{-1} \begin{pmatrix} A_1^t M^{-1} w_1 \\ \\ -w_2 \end{pmatrix} \qquad (23)$$

672

$$k_1 = -M^{-1}(A_1 \Delta x + w_1);$$

$$\Delta l = Q(B k_1);$$

$$\hat{\sigma}^2 = \frac{\Delta l^t P \Delta l}{r - u + s};$$

$$Q = P^{-1}; \quad M = B^t Q B; \quad N = A_1^t M^{-1} A_1; \quad w_2 = A_2^t \overset{\circ}{x};$$

This is a nonlinear problem, why the process has to be iterated until Δx^{i+1} is less than a certain selected limit. For each iteration, then new parameters are computed by

$$\hat{x}^{i+1} = \hat{x}^i + \Delta x^{i+1} \qquad (24)$$

4. TESTS

The main discussion concerns the critical geometric situation where a straight line under observation lies in the same plane as the projection centres of the image pair. The situation makes it impossible to calculate the line parameters. This is also known as the epipolar case.

In the test we do not use the angle in the image between the line and the epipolar plane. Instead the angle between the direction vector d and the difference vector b of the two image projection centres in object space is used as an approximation. In the following, this angle is called EPI. Several image combinations have been chosen to give a wide variation of the angle EPI, i.e. between 0 and 100 gon. The result from tests where more than two images have been used is not dependent of the epipolar case. Also the influence from the geometric constraints on the resulting line parameters, i.e. vertical and horizontal, are checked. Test results are shown in column diagrams, where black is used to represent results where no geometric constraints have been used. White represents results with geometric constraints. The origo of the ground coordinate system has been moved into the approximative centre of each building. This is done to achieve a better numerical stability. Two buildings, A and B, are used in the tests. Building A is projected in five and building B in four images.

4.1 Separate lines

All lines of the two test buildings were calculated using a) measurements from all available images which gives a result independent of the angle EPI and b) measurements using image pairs.

It is assumed that the changes of the angle EPI is one of the most important factors influencing the precision and reliability of the calculated 3D lines in case b. Therefore all estimated a posteriori standard deviations of the adjusted line parameters are presented in relation to the variations of the EPI-angle.

The standard deviations of the angles δ, φ, γ do not have the same units and dimensions, as the metric distance r why the results are presented separately.

Figure 3 show the mean of the standard deviations of the three angles δ, φ, γ for test case a described above where each line of building A and B is shown separately. One result from figure 3 is that geometric constraints leads to a reduction of the standard deviations. The standard deviations of the angles of the horizontal lines, which are line 1 to 6 for building A and 1 to 4 for building B, are not as much decreased as the standard deviations of the vertical lines. On the other hand the standard deviations for the metric parameter r does not give a much better result when geometric constraints are introduced as shown in figure 4. These results are independent of the angle EPI.

Figures 5 and 6 show the results from the test case b. The mean of the standard deviation of the angle δ, φ, γ is plotted as a function of angle EPI. This is done to see if it is possible to derive a logarithmic function which can describe the variation of the calculated standard deviations as a function of angle EPI.
An examination of the approximate logarithmic curves in figure 5 shows, that the introduction of the horizontal constraint decrease the mean of the standard deviations of the angles with approximately power of one, especially for building B. Without geometric constraint the mean values increase significant, if the angle EPI becomes less than about 25 gon. Figure 5 shows that. The introduction of the horizontal constraint do not result in different standard deviations for parameter r.

4.2 Combination of straight lines

The same measurements and results from the adjustment process are used as in the previous section. Results from using stereo photogrammetry and monoscopical line photogrammetry will be compared with each other and with the results achieved using a geodetic measuring method.

The subject of the investigation are horizontal distances between and height differences of the corner points of the two test buildings. The coordinates of the corner points are directly measured using stereo photogrammetry. In line photogrammetry the corner points are defined as the point of gravity of those vectors, which are the shortest connection between the calculated 3D straight lines.

The geodetic system, which is used as reference system, is based on a local coordinate system. Thus the high precision of this method is prevented. The two photogrammetric methods are based on the official ground coordinate system. Therefore horizontal distances and the differences of the corner point heights to the mean height of each building are compared, instead of the 3D point coordinates.

Horizontal distances   The distance s_{ij} between two corner points i, j are calculated as

$$s_{ij} = \sqrt{(X_i - X_j)^2 + (Y_i - Y_j)^2} \qquad (25)$$

The differences for each distance to the reference system are calculate by

$$\Delta_{g,s} = s_{ij}^{geod} - s_{ij}^{stereo} \qquad (26a)$$

$$\Delta_{g,l} = s_{ij}^{geod} - s_{ij}^{line} \qquad (26b)$$

$\Delta_{g,s}$ is the difference between geodetic distances and distances calculated by stereo measurements. $\Delta_{g,l}$ is the difference between geodetic distances and distances calculated by line photogrammetry. The horizontal distances based on the geodetic measurements are assumed to be "true". The empirical standard deviation of the distances are

$$\sigma_\Delta = \sqrt{\frac{\sum(\Delta^2)}{n}} \qquad (27)$$

The number of horizontal lines is denoted n and not (n-1) because of the assumption that the geodetic distances are "true" values.

The horizontal lines of the two buildings are pairwise perpendicular to each other. Therefore always two EPI angles for a image pair exist and are used. Figure 7 shows σ_Δ for different angle combinations. The angle combinations 10/91, 17/84 gon for building A without constraint and the combination 15/83 gon for building B are about two to three times larger as the other ones. A check of the "all"-column shows, that the use of more than two images only result in decreased standard deviations, if angle EPI is less than about 25 gon compared to image pairs. Otherwise the calculated empirical standard deviations are the same.

The results based on stereo measurements are presented in figure 8. For building A, they are about twice as large as those using line photogrammetry with constraints. The standard deviations for building B have about the same size for both methods, i.e. ±7 cm.

Height differences of the corner points The roofs of the two test buildings are horizontal, this is proofed with the help of the geodetic method. The mean heights are calculated by using the heights of all corner points for each of the two buildings. This is done for stereo and line photogrammetry. The empirical standard deviation of the height of the corner points is calculated as following:

$$\sigma_\Delta = \sqrt{\frac{\sum(\Delta_h^2)}{n-1}} \qquad (28)$$

$$\bar{Z} = \frac{\sum Z_i}{n} \quad ; \quad \Delta_h = \bar{Z} - Z_i$$

where n is the number of the corner points, $\bar{Z}$ is the mean height and Z_i the height of point i.

For building A the influence of angle EPI on the standard deviation of the height differences is only detectable, if no geometric constraint is introduced Figure 9a. For the angle combinations 10/91 gon and 17/84 gon the standard deviations without constraints are more than three times as large as those with introduced constraint. Otherwise the standard deviations for small angles is less than for those with large angles and for them using all images. Figure 10a shows, that all results from the stereo measurement, with the exception of model 1/2 shows a larger empirical standard deviation compared to those calculated by line photogrammetry.

The empirical standard deviations calculated using line photogrammetry for building B, in figure 9b, are less dependent of the angle EPI compared to the same values for building A. Comparing the results from line photogrammetry (figure 9b) with stereo photogrammetry, shown in figure 10b, are almost the same. In figures 8, 10 the column underlined with "mean" is a mean value calculated by using all results from the stereo measurements.

5. DISCUSSION

All tests were based on real data. The results are therefore influenced by several different kinds of errors. Nevertheless clear tendences in respect to the variations of the angle EPI are shown. This is also valid for the introduction of geometric constraints, when image pairs, as well as multi images are used.

The check of the plotted logarithmic functions, in figures 5 and 6, shows that it is not possible to establish a general relation, which could predict the change of the standard deviations in respect to a variation of angle EPI, with an acceptable fidelity. The standard deviations of the parameters δ, ϕ, γ become considerably smaller, if geometric constraints are introduced and angle EPI is less than about 25 gon, this is visible in figures 5. The same is valid for the standard deviations of the differences of horizontal distances (figures 7). This allows the inference, that the introduction of a horizontal constraint causes an improvement of the estimated planimetric position of a straight line. This is not valid for the height values.

The precision of the Z-component increases strongly, if the angle EPI is less than about 25 gon. This is estimable when calling in mind that a 3D straight line cannot be estimated if it lies parallel to the connection of the two projection centers, i.e. when the epipolar angle is zero. This is also a reason, that the planimetric position is more robust as the height values with respect to a small angle EPI.

The results achieved by line photogrammetry are more precise as those from stereo photogrammetry, if the angle EPI is larger than about 25 gon, or if the measurements from all images are used. The validity of this statement is not so strong, as it is only based on a small amount of data. More extensive tests are needed to achieve a more reliable result.

We expect, that the introduction of intersection constraints into the adjustment process will result in more

674

precise and reliable 3D line parameters, especially for those lines which are nearly parallel to the epipolar plane, as their position in 3D will be fixed through the intersection with other lines in two line points.

The introduction of a local coordinate sytem for the geodetic method caused that no absolute coordinates could be compared. The organisation of further tests should be done in such a way, that this is possible. A further point of criticism is, that not the real epipolar angle in image space was used but an approximation, the angle EPI. Therefore it was not possible to check the vertical lines in respect to the variation of the epipolar angle.

Our opinion is, that line photogrammetry can be used with advantage as a tool for the calculation of man-made objects after semi- or fully automatic localisation of such objects in digital images. Therefore, and caused by the promising results achieved in the tests done here, investigations concerning the extraction of image points for line photogrammetry using matching or other segmentation methods in digital images will be done in the future. Furthermore, all theoretically derived constraints will be implemented and more complex features will be tested in respect to their applicability for this method.

6. ACKNOWLEDGMENTS

7. REFERENCES

1 Lugnani, J. B., 1982. The Digitized Features - A New Source of Control. In: Int. Congress of Photogrammetry and Remote Sensing., Taniemi-Japan, Vol. XXIV Supplement, pp. 188 - 202

2 Masry, S. E., 1981. Digital Mapping Using Entities: A New Concept. Photogrammetric Engineering and Remote Sensing. Vol 48(11): 1561-1599.

3 Mulawa, D. C., Mikhail, E.M., 1988. Photogrammetric Treatment of Linear Features. In: Int. Congress of Photogrammetry and Remote Sensing., Kyoto-Japan, Vol. 27 Part B10, pp. 383 -393.

4 Persson, B., 1985. Linjefotogrammetri. Department of Photogrammetry, Royal Institute of Technology, Stockholm Sweden. Unpublished.

5 Sayed, A. N., Mikhail, E.M, 1990. Extraction And Photogrammetric Exploitation Of Features In Digital Images. Report CE-PH-90-7, School Of Civil Engineering, Purdue University, West Lafayette, USA

8. FIGURES
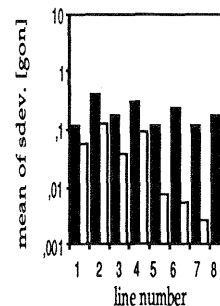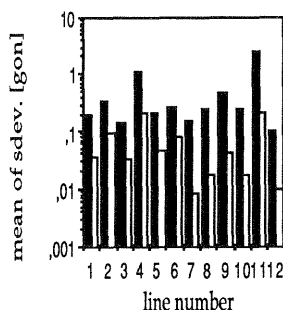
Figure 3a: Figure 3b:

Figure 3a and 3b shows the results from test case a for building A and B respectively The columns show the mean of the standard deviation of the estimated angles δ, φ, γ with (black) and without (white) the introduction of the geometric constraints. Line 1 to 8 of building A and line 1 to 4 of building B are horizontal. The vertical lines are line 7 to 12 for building A and 5 to 8 for building B.
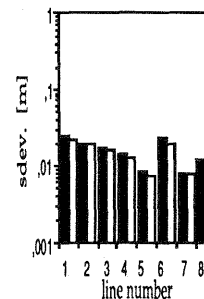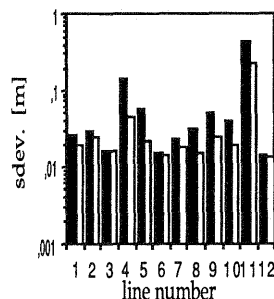
Figure 4a: Figure 4b:

Figures 4a and 4b shows the same test case as shown in 3a and 3b, but with the standard deviations of the estimated metric parameter r instead of the angles δ, φ, γ.
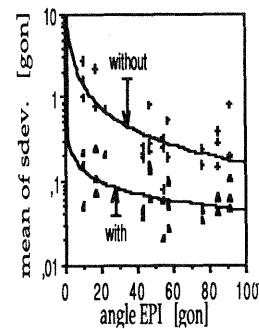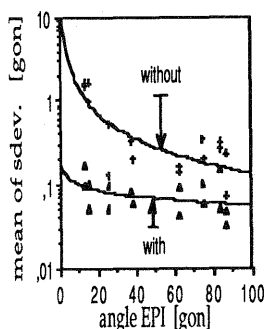
Figure 5a   Figure 5b:

Figure 5a and b: Measurements from test case b where the mean of the standard deviations of the angles δ, φ, γ are plotted, as a function of angle EPI. Results without geometric constraints are plotted using crosses (+) and triangels (Δ) are used for cases with constraints.
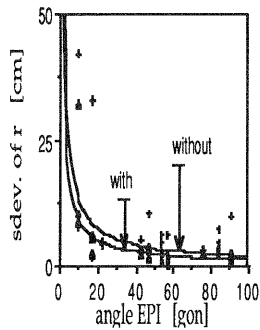
Figure 6a

Figure 6b

Figure 6a and 6b show the same results as figure 5a and 5b but with the standard deviation of the estimated metric parameter r instead of δ, φ, γ.
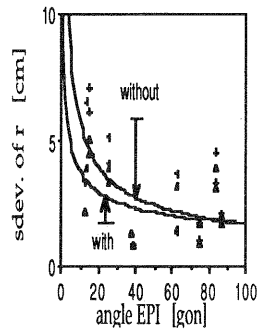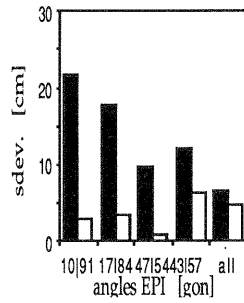
Figure 9a:

Figure 9b:

Figure 9a and 9b shows the standard deviations of the height differences of the corner points of building A (9a) and building B (9b) in respect to different combinations of angle EPI. Results without (dark) and with (white) geometric constraint are presented.
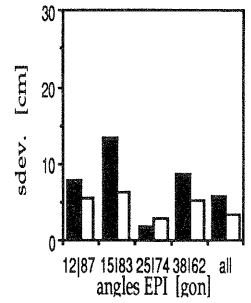
Figure 7a
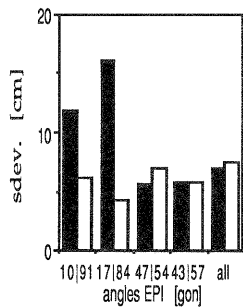
Figure 7b

Figure 7 shows the standard deviations of the horizontal distances between corner points of building A (7a) and building B (7b) in respect to different combinations of angle EPI. Results without (dark) and with (white) constraints are presented.
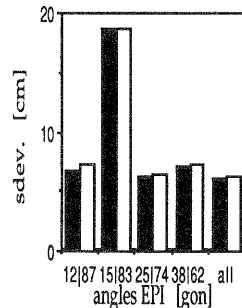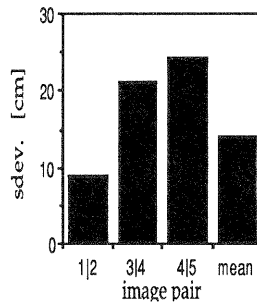
Figure 10a:

Figure 10b:

Figure 10a and 10b show the standard deviations of the height differences for building A and B. The results of the first three columns of figure 10a (building A) and the first two columns of figure 10b (buidling B) are calculated based on one stereo model. The last column of the figures present the mean value calculated using all stereoscopically measured data.
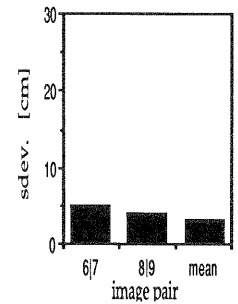
Figure 8a:
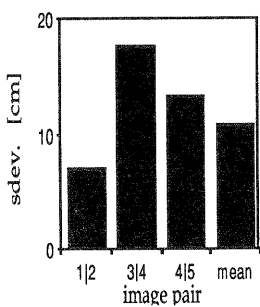
Figure 8b:

Figure 8a and 8b show the standard deviations of the horizontal distances between the corner points of building A and B. The results of the first three columns of figure 8a (building A) and the first two columns of figure 8b (building B) are calculated based on the data from one stereo model. The last column of the figures present the mean value calculated using all measured image data.